Radiation Physics and Chemistry 223 (2024) 111970

Contents lists available at ScienceDirect

Radiation Physics and Chemistry

journal homepage: www.elsevier.com/locate/radphyschem

Small field dosimetry employing the thermoluminescence technique using a 3D printed phantom

S.B. Almeida [a,*], A.P.V. Cunha [b], P.V.S. Tavares [a], C.C. Sampaio [b], G. Menegussi [b], L.L. Campos [a]

[a] Radiation Metrology Center, Instituto de Pesquisas Energéticas e Nucleares, Av. Prof. Lineu Prestes, 2242 – Cidade Universitária, São Paulo, SP, Brazil
[b] Radiation Therapy Department, Hospital das Clínicas de São Paulo – HC, Av. Dr. Enéas Carvalho de Aguiar, 255, Cerqueira César, São Paulo, SP, 05403-000, Brazil

ARTICLE INFO

Handling Editor: Dr. Chris Chantler

Keywords:
Radiotherapy
Dosimetry
Small field
Dosimeters thermoluminescent
3D printed
Stereotactic radiosurgery

ABSTRACT

With the advent of new radiotherapy modalities, it has become necessary to apply relatively small fields that are dynamic or static. The use of these field sizes can cause uncertainty in dosimetry, requiring special attention in small field dosimetry. With these mentioned challenges, it is difficult to select a detector with good performance for dosimetry in small fields. TLDs have advantages because they have characteristics such as high spatial resolution and dose response, they offer a promising opportunity to measure the absorbed dose in a small field. The objective of this study is to evaluate the performance of $CaSO_4$:Dy, LiF:Mg,Ti and μLiF:Mg,Ti thermoluminescent dosimeters for clinical photon beams in small field dosimetry using a 3D printed phantom. For clinical application the 6EX linear accelerator from Varian Medical System and the Multillif collimator from BrainLab were used. The 3D printed phantom was subjected to real treatment conditions. The dynamic arc 3D radiosurgery technique was adopted, with a dose of 7 Gy. To decrease statistical variation, the treatment simulation was repeated three times for each dosimeter. The results obtained demonstrated the viability of TLDs for clinical applications from photon beams to small fields. The values showed agreement in percentage terms below ±5% as recommended by the ICRU. The greatest percentage difference found was 1.2% (LiF:Mg;Ti) in relation to the planning system. All thermoluminescent dosimeters presented an uncertainty relatively low, with good stability and reproducibility in all measurements. The 3D printed phantom showed the possibility of achieving real treatment conditions.

1. Introduction

Stereotactic radiosurgery (SRS) is characterized by a single dose treatment or fractional ionizing radiation to treat intracranial lesions and the characteristics of the planning involve a sharp dose gradient at the periphery of the target, seeking preserve healthy tissue around the lesion (Crompton et al., 2023; Foster et al., 2023; Niranjan et al., 2019; XU et al., 2022). In radiotherapy, the new techniques have some difficulties, such as: dosimetry of the beam, geometric characterization, and the use of small radiation fields (Alfonso et al., 2008). In some cases, field sizes are reduced because the lesions are well small, treatment simulations in planning play a very important role, in this way, they must be provided with data referring to these small fields. Dosimetry becomes quite complex, as precision becomes quite questionable, especially when small fields are being used in regions of low density (Das et al., 2008, 2022).

The use of small fields in radiotherapy techniques has increased substantially, especially in stereotaxic treatments, where uniform or non-uniform fields are used, making it possible through the intensity modulated radiotherapy technique that can modulate the radiation beam in minimum dimensions. This technology was facilitated by the increased availability of Brainlab's M3 multileaf collimators, which make it possible to reduce the field size depending on the size of the lesion. However, for these fields, dosimetric errors became considerably greater than in conventional fields, this was mainly due to two reasons: (a) the reference conditions recommended by conventional Codes of

* Corresponding author.
E-mail address: shirlane02@gmail.com (S.B. Almeida).

https://doi.org/10.1016/j.radphyschem.2024.111970
Received 1 March 2024; Received in revised form 18 June 2024; Accepted 20 June 2024
Available online 21 June 2024

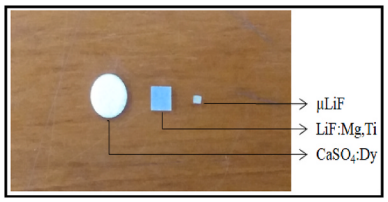

Fig. 1. Thermoluminescence dosimetry.

Practice (CoP) cannot be established on some machines and (b) measurement of absorbed dose in water in composite fields is not standardized (Alfonso et al., 2008; Palmans et al., 2018).

To develop standardized recommendations for dosimetry detectors and procedures, an international working group on small and non-standard field reference dosimetry has been established by the International Atomic Energy Agency (IAEA) in cooperation with the AAPM who have published a new TRS- 483, with recommendations for clinical reference dosimetry based on absorbed dose in water (Palmans et al., 2018).

With these challenges mentioned, it is difficult to select a detector that performs well in small fields. The required properties of a desired detector are high spatial resolution, high signal (low noise), low energy dependency, low directional dependency, water equivalence, high stability, and clinical ease of use. Of course, there is no default detector for small fields, because no detector has all the properties. However, some detectors that are recommended by the TRS - 483 are used, such as: ionization chambers, thermoluminescent dosimeters (TLDs), polymer gels, field effect transistors, metal oxide semiconductors (MOSFETs), diamond detectors, silicon diodes, dosimeters alanine, and Monte Carlo (MC) simulations, among others (Palmans et al., 2018; Parwaie et al., 2018).

The thermoluminescent (TL) dosimeters have the advantage of presenting characteristics such as high spatial resolution and linear dose response, offering a promising opportunity to measure the absorbed dose in a small field. The μLiF dosimeters have shown great feasibility in this type of application and can be applied to determine the dose in a region based on its size, that is, 1 mm × 1 mm ×1 mm. The size of these TLDs is a limitation on their accuracy in places where the dose can vary rapidly between regions separated by small distances. Another type of TLD is the TLD-100, which has a linear dose response that is also recommended for this type of application (Palmans et al., 2018; Parwaie et al., 2018).

2. Materials and methods

The detectors (LiF:Mg;Ti, μLiF:Mg;Ti and $CaSO_4$:Dy) in this study were selected based on their sensitivity, response linearity, reproducibility, physical dimensions, and availability for use clinical in small fields (Fig. 1).

2.1. Heat treatment system

- Vulcan® muffle furnace, model 3–550 PD, from LMD/IPEN;

  $CaSO_4$:Dy – 300° for 3 h;
  LiF:Mg;Ti, μLiF:Mg;Ti – 400° for 1 h.

- Drying and sterilization oven, model SL-100, from LMD/IPEN.

  LiF:Mg;Ti, μLiF:Mg;Ti – 100° for 2 h.

2.2. TL reading system

- TL reader from HarshawTM brand, model 4500 from Thermo Scientific of LMD/IPEN – ($CaSO_4$:Dy);
- TL/OSL reader from RISOTM, model TL/OSL-DA-20 from LMD/IPEN – (LiF:Mg;Ti, μLiF:Mg;Ti).

2.3. Phantoms

- SW solid water plates measuring 30 × 30 × 1 cm^3, Hospital of Clínicas FMUSP/INRAD;
- SW solid water plate measuring 30 × 30 × 0.5 cm^3, Hospital of Clínicas FMUSP/INRAD;
- Skull Phantom 3D printed, from LMD/IPEN.

2.4. Irradiation and image acquisition systems

- ^{137}Cs gamma radiation source, 4π geometry with activity of 38.11 GBq on April 17, 2014 from the Thermoluminescent Dosimetry Laboratory (LDT/IPEN);
- Clinac 6 EX Linear Accelerator from Varian, belonging to the Hospital of Clínicas FMUSP/INRAD;
- GE 4-channel computed tomography machine, belonging to the Hospital of Clínicas FMUSP/INRAD;
- Exctrac System, belonging to Hospital of Clínicas FMUSP/INRAD.

The selection of $CaSO_4$:Dy detectors was based on the TL sensitivity to ^{137}Cs gamma radiation, under electronic equilibrium conditions. The LiF:Mg,Ti and μLiF:Mg,Ti detectors were irradiated using the RISOTM Sr 90/Y 90 irradiation source. All detectors showed a variation of less than 5% for each type detector, and the repeatability and reproducibility of their TL response were investigated. For this study, 12 dosimeters of each type were used.

Dosimetric characterization was performed using a Varian's Clinac 6 EX linear accelerator. For this procedure, six solid water plates 1 cm thick and one plate 0.5 cm thick and a BrainLab M3 multileaf collimator were used. The dosimeters were irradiated with energy of 6 MV in the dose range of 0.8 Gy–10 Gy. Beam calibration was performed according to TRS 398.

The skull phantom was developed from a prototype of the CIRS 711 simulator, using two types of filaments equivalent to soft tissue (PLA) (Almeida, 2022; Almeida et al., 2017) and bone tissue (ABS XCT-A) (Savi et al., 2020). The 3D printed skull phantom has characteristics capable of simulating a patient undergoing SRS treatment.

For clinical application, the 3D printed phantom was subjected to real simulation and radiotherapy planning conditions. A type B stereotaxic thermoplastic mask (Oxigen) was manufactured for extereotactic radiosurgery treatment, and then a computed tomography scan of the phantom was performed for radiotherapy planning (Fig. 2). After the planning process, the 3D printed simulator was subjected to real

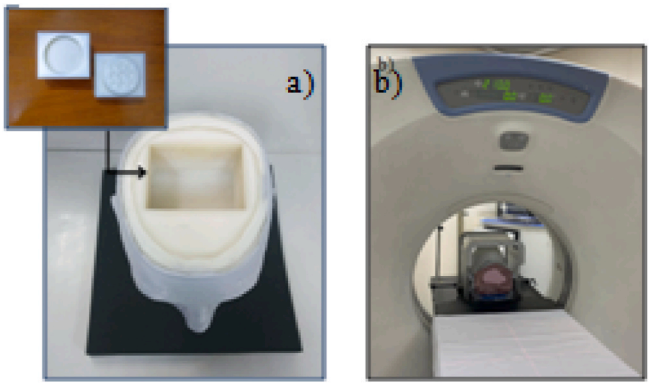

Fig. 2. a) Accessory to insert DTLs in the phantom 3D printed. b) CT phantom with thermoplastic mask.

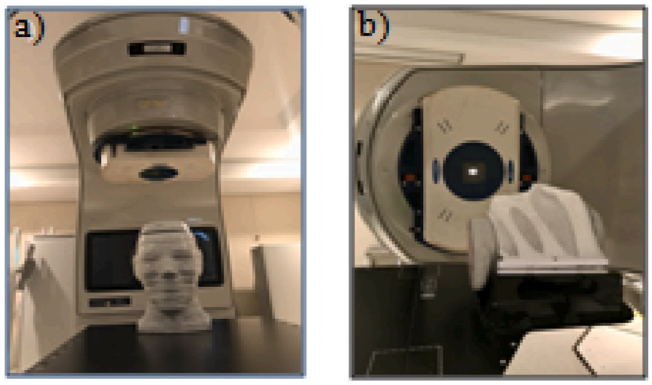

Fig. 3. a) Phantom 3D printed, b) Positioning the phantom with the thermoplastic mask for radiosurgery.

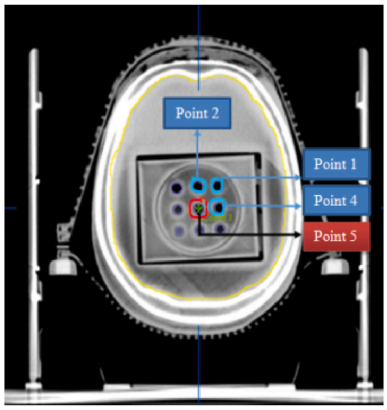

Fig. 4. Tomographic image of the phantom in axial section with structure delineation.

treatment conditions using the 6EX linear accelerator from Varian Medical System and the Multillif collimator from BrainLab. The 3D radiosurgery technique with dynamic arc was adopted, with a dose of 7 Gy (Fig. 3). The Exactrac® system was used according to radiosurgery protocol. To reduce statistical variation, the treatment simulation was repeated three times for each dosimeter group (the same dosimeter being used for each irradiation point). Fig. 4 demonstrates the distribution of dosimeters inside the phantom and how the planning was carried out. The target volume defined for treatment was the brain. Point 5 was defined as the PTV with a treatment field size 1.4 × 1.5 cm. Organs at risk were defined as tissues close to the PTV.

3. Results and discussions

3.1. Dose response curves

The dose response curve is defined as the relationship of the radiation dose absorbed by the detector and the intensity of the TL response. For the dosimetric material, the ideal would be for it to present a linear dose-response over a wide dose range. The behavior of the curve appears linear from the lower limit of detection to a region where the amount of light emitted increases faster and this region is called supralinearity. For doses with higher values, the TL response may saturate, thus reducing the sensitivity of the dosimeter (Almeida, 2017; Mckeever et al., 1995). The dose-response curves are shown in Fig. 5. Each value presented on the curves representes the average of the three TL readings. The dose response curves for clinical photon beams for LiF:Mg;Ti, and μLiF:Mg;Ti dosimetry showed a linear behavior up to 2 Gy and for doses higher than 4 Gy the results show a tendency towards supralinearity. For $CaSO_4$:Dy dosimeters, the TL response showed linearity for doses of up to 6Gy, showing supralinearity from dose of 8Gy onwards.

Due to the detector's behavior showing supralinearity at doses above 4 Gy, it was necessary to use the calibration factor (Fcal. Relative to dose of 0,8Gy (Gy/μC)) for individual doses. The calibration factor values are presented in Tables 1–3.

3.2. Clinical applications

Clinical applications were carried out according to the radiosurgery treatment protocol. The phantom adopted real treatment conditions including performing X-ray imaging for each treatment field as performed in radiotherapy departments. The IGRT technique is widely applied in treatments that use high doses of radiation in few fractions. Exactrac® is an X-ray-based monitoring system, this technology ensures submillimeter precision during radiosurgery treatment regardless of the table angle or gantry position.

The TL response values of each detector and the TPS (Planning system) dose values are described in Tables 1–3 below.

The results obtained demonstrated the viability of TLDs for applications small field photon beam clinics. The values described in the tables above show agreement in percentage terms below ±5% as recommended by ICRU. The largest percentage difference found was 1.2% (LiF:Mg,Ti) in relation to the PTV planning system. All named points (OAR) presented doses lower than the planning system, with the largest percentage difference being 31.5% (LiF:Mg,Ti) demonstrating the quality of collimation of the radiation beam to the tissues adjacent to the PTV. All thermoluminescent dosimeters showed a relatively low uncertainty, with good stability and reproducibility in all measures. Thus, according to this analysis in relation to the iPlan® planning system, dosimeters highlighted the tissue equivalence of the 3D printed phantom. Same presenting some factors that impacted its construction, such as the presence of air in its interior due to the warp effect and material deposition failures in some parts (Fig. 6). The phantom showed the possibility of achieving real treatment conditions. This one result is quite considerable considering the importance of clinical dosimetry in radiotherapy departments, as it can make a comparison between doses provided by the planning system with the doses evaluated by the dosimeters (detectors). The present study enabled accessible dosimetric methodologies in view of the difficulties of measuring and evaluating doses in small fields, providing the use of thermoluminescent dosimeters as support dosimetry for small fields.

The phantoms are of fundamental importance for quality control in radiotherapy departments, playing an essential role in determining the dose delivered to the patient, as it can be subjected to real treatment conditions, proving its effectiveness in determining various factors that may cause some type of error in the prescribed dose.

The 3D printed phantom has characteristics close to human tissue, providing dosimetry in conditions like a real treatment. Despite presenting some printing flaws and having air inside it caused by the warp effect, the phantom presented excellent viability for clinical application and did not have a significant impact on measurements carried out with thermoluminescent dosimeters.

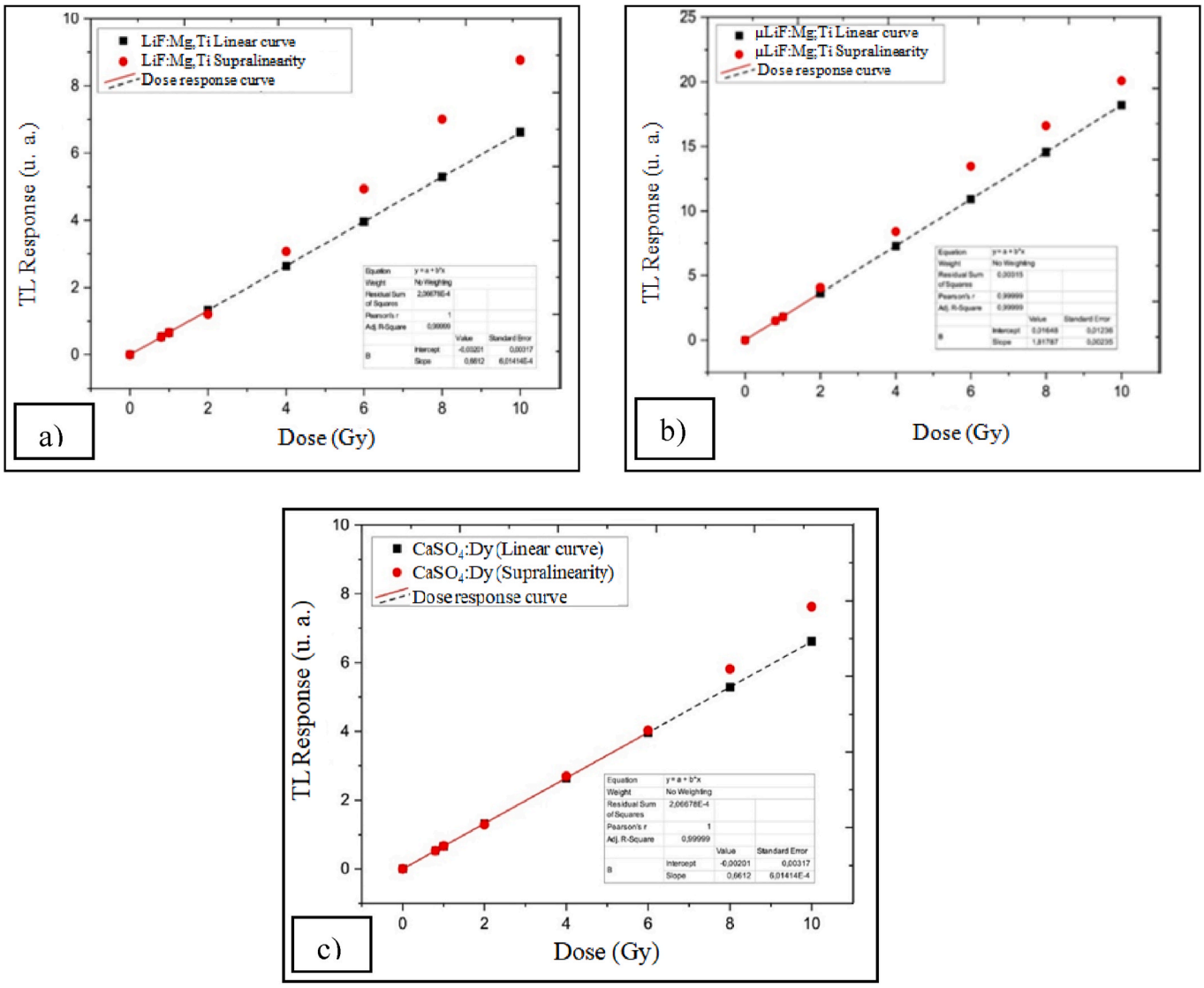

Fig. 5. Dose Response Curves – a) LiF:Mg;Ti, b) μLiF:Mg;Ti e c) $CaSO_4$:Dy.

Table 1
($CaSO_4$:Dy) Doses evaluated in the 3D printed skull phantom compared to the planning system.

Spot	Resp. TL (μC)	Fcal. Rel. 0,8Gy (Gy/μC)	Evaluated dose (Gy)	Dose Planning (Gy)	SDM (Gy)	CV%	Dif. %
1(OAR)	2.45	0.151	0.37	0.44	0.01	2.7	15.9
2 (OAR)	9.74	0.151	1.47	1.62	0.01	0.7	9.3
4 (OAR)	8.77	0.151	1.32	1.80	0.03	2.3	26.7
5 (PTV)	59.67	0.137	8.20	8.12	0.04	0.5	1.0

*OAR – Organ at risk, PTV – Target planning volume; SDM - standard deviation of the mean; CV - coefficient of variation.

Table 2
(LiF:Mg;Ti) Doses evaluated in the 3D printed skull phantom compared to the planning system.

Spot	Resp. TL (Count)	Fcal. Rel. 0,8Gy (Gy/Count)	Evaluated dose (Gy)	Dose Planning (Gy)	SDM (Gy)	CV%	Dif. %
9 (OAR)	46,110	1.212	0.55	0.57	0.01	1.8	3.5
8 (OAR)	88,916	1.212	1.08	1.34	0.03	2.7	19.4
6 (OAR)	100,956	1.212	1.22	1.78	0.04	3.2	31.5
5 (PTV)	720,287	0.114	8.22	8.12	0.15	1.8	1.2

*OAR – Organ at risk, PTV – Target planning volume; SDM - standard deviation of the mean; CV - coefficient of variation.

Table 3
(μLiF:Mg;Ti) Doses evaluated in the 3D printed skull phantom compared to the planning system.

Spot	Resp. TL (Count)	Fcal. Rel. 0,8Gy (Gy/Count)	Evaluated dose (Gy)	Dose Planning (Gy)	SDM (Gy)	CV%	Dif. %
1 (OAR)	66,280	0.526	0.35	0.39	0.01	2.9	10.3
2 (OAR)	183,436	0.526	0.96	1.00	0.02	2.1	4.0
5 (PTV)	1,713,373	0.048	7.92	7.89	0.02	0.3	0.4

*OAR – Organ at risk, PTV – Target planning volume; SDM - standard deviation of the mean; CV - coefficient of variation.

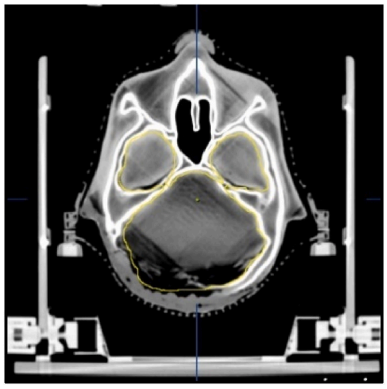

Fig. 6. Axial computed tomography image of the 3D printed phantom demonstrating deposition failure of the PLA material.

4. Conclusions

The results obtained demonstrate that, although the manipulation and evaluation procedure of TLDs is time consuming and requires careful attention, it is possible to achieve accuracy in measurements small field dosimetry in clinical photon beams.

In view of the difficulty in measuring and evaluating doses in small fields, thermoluminescent dosimeters presented excellent results in clinical dosimetry, proving to be an effective detector for support dosimetry in small fields.

We can conclude that with the use of the 3D phantom with the thermoluminescent dosimeters proved to be very useful in the application of small field dosimetry, allowing a more precise investigation in the quality controls involving treatments whose doses are relatively high in techniques such as radiosurgery.

CRediT authorship contribution statement

S.B. Almeida: Writing – original draft, Validation, Resources, Project administration, Methodology, Investigation, Formal analysis. **A.P.V. Cunha:** Supervision. **P.V.S. Tavares:** Software. **C.C. Sampaio:** Methodology. **G. Menegussi:** Supervision. **L.L. Campos:** Supervision, Project administration.

Declaration of competing interest

The authors declare that they have no known competing financial interests or personal relationships that could have appeared to influence the work reported in this paper.

Data availability

No data was used for the research described in the article.

Acknowledgment

FAPESP Proc. No. 2018/05982-0 and CNPq Proc. No. 426513/2018-5.

References

Almeida, S.B., 2022. Dosimetric Evaluation Using Thermoluminescent Materials and Development of an Anthropomorphic Simulator of the Skull Printed in 3D for Small Field Dosimetry Using Clinical Photon Beams. Doctoral dissertation, Universidade de São Paulo.

Almeida, S.B., 2017. Validation and Dosimetric Evaluation Employing the Techniques of TL and OSL of Thermoluminescent Materials for Application in the Dosimetry of Clinical Beams of Electrons Used in Total Irradiation of the Skin – TSI. Doctoral dissertation, Universidade de São Paulo.

Almeida, S.B., Valeriano, C.C.S., Campos, L.L., 2017. Evaluation of replacing PMMA plates with 3D printed PLA on the TL response of $CaSO_4$: Dy. Braz. J. Radiat. Sci. 5, 3–A. https://doi.org/10.15392/bjrs.v5i3-A.295.

Alfonso, R., Andreo, P., Capote, R., Huq, M.S., Kilby, W., Kjäll, P., et al., 2008. A new formalism for reference dosimetry of small and nonstandard fields. Med. Phys. 35 (11), 5179–5186. https://doi.org/10.1118/1.3005481.

Crompton, D., Koffler, D., Fekrmandi, F., Lehrer, E.J., Sheehan, J.P., Trifiletti, D.M., 2023. Preoperative stereotactic radiosurgery as neoadjuvant therapy for resectable brain tumors. J. Neuro-oncol. 165 (1), 21–28. https://doi.org/10.1007/s11060-023-04466-5.

Das, I.J., Ding, G.X., Ahnesjö, A., 2008. Small fields: nonequilibrium radiation dosimetry. Med. Phys. 35 (1), 206–215. https://doi.org/10.1118/1.2815356.

Das, I.J., Dogan, S.K., Gopalakrishnan, M., Ding, G.X., Longo, M., Franscescon, P., 2022. Validity of equivalent square field concept in small field dosimetry. Med. Phys. 49 (6), 4043–4055. https://doi.org/10.1002/mp.15624.

Foster, R.D., Moeller, B.J., Robinson, M., Bright, M., Ruiz, J.L., Hampton, C.J., Heinzerling, J.H., 2023. Dosimetric analysis of intra-fraction motion detected by surface-guided radiation therapy during Linac stereotactic radiosurgery. Adv. Radiat. Oncol. 8 (3), 101151 https://doi.org/10.1016/j.adro.2022.101151.

Mckeever, S.W.S., Moscovitch, M., Townsend, P.D., 1995. Thermoluminescencedosimetry Materials: Properties and User. Nuclear Technology Publishing, Ashford, Kent.

Niranjan, A., Kano, H., Monaco III, E.A., Lunsford, L.D., 2019. Salvage Leksell Stereotactic Radiosurgery for Malignant Gliomas. In: Leksell Radiosurgery, vol 34. Karger Publishers, pp. 191–199. https://doi.org/10.1159/000493064.

Palmans, H., Andreo, P., Huq, M.S., Seuntjens, J., Christaki, K.E., Meghzifene, A., 2018. Dosimetry of small static fields used in external photon beam radiotherapy: summary of TRS-483, the IAEA–AAPM international Code of Practice for reference and relative dose determination. Med. Phys. 45 (11), e1123–e1145. https://doi.org/10.1002/mp.13208.

Parwaie, W., Refahi, S., Ardekani, M.A., Farhood, B., 2018. Different dosimeters/detectors used in small-field dosimetry: pros and cons. J. Med. Sign. Sens. 8 (3), 195. https://doi.org/10.4103/jmss.JMSS_3_18.

Savi, M., Andrade, M.A.B., Potiens, M.P.A., 2020. Commercial filament testing for use in 3D printed phantoms. Radiat. Phys. Chem. 174, 108906 https://doi.org/10.1016/j.radphyschem.2020.108906.

Xu, Q., Huynh, K., Nie, W., Rose, M.S., Chawla, A.K., Choe, K.S., et al., 2022. Implementing and evaluating a high-resolution diode array for patient-specific quality assurance of robotic brain stereotactic radiosurgery/radiotherapy. J. Appl. Clin. Med. Phys. 23 (5), e13569 https://doi.org/10.1002/acm2.13569.